

# Mechanical characteristics of geosynthetic-enveloped soils

K. Makiuchi, Y. Kawaguchi & K. Minegishi  
*College of Science & Technology, Nihon University, Japan*

**ABSTRACT:** A fundamental study was made on the confining effects of geosynthetic-enveloped noncohesive soils. A series of uniaxial compression tests was carried out on a cylindrical specimen of dry fine sand compacted within three types of hollow-shaped geononwovens and their axial and radial stress-strain relationships were investigated. The test results demonstrated the marked improvement of the mechanical characteristics such as modulus of deformation, compressive strength associated with reductions in their strain at failure. A mechanism of mobilization of confining radial pressure and deformation restraint was discussed and the estimation methods of an apparent cohesion of geocapsulated granular soil were presented. The confining effects depend on the tensile properties of geotextiles, the relative density of soil and so forth.

## 1 INTRODUCTION

One of the most distinctive functions of geosynthetics as an earth reinforcement is to restrain a deformation or to apply a circumferential confinement pressure to soil mass. In fact, geosynthetic-enveloped soil systems, such as sandbag, tubular bag, gabion, geocapsule, geocell, geomattress, semi-enveloped geotextile-facing of slope embankment and others, are widely adopted on site as traditional and effective methods. The motivation for this study was provided by the need to advance fundamental knowledge about the characteristics of those geosynthetic-enveloped soils.

A series of laboratory element and model tests has been conducted so far regarding to geocapsules using several reinforcing materials such as geononwoven, geowoven, papers and rigid mould for cohesionless and cohesive soils. In this paper the results of uniaxial compression tests on a cylindrical geononwovens-enveloped sand specimen are presented in order to investigate the effects of tensile properties of geosynthetics and the relative density of sand on their axial

and radial stress-strain relationships. A mobilization of restraint of geotextile-enveloped sand is reviewed and the approaches to make the quantitative evaluation of the restraint effects are discussed in detail.

## 2 EXPERIMENTAL TECHNIQUES

Three types of geononwovens having different thicknesses were employed for the experiment works and their tensile strength and elongation at breaking are shown in Table 1. These geotextiles were sewn together in the form of hollow cylinder of 10 cm in diameter and 10 cm in height. The soil used for the test is Toyoura fine sand in the air dry condition. The diameter of 60% passing  $D_{60}$  is 0.2 mm, the density of soil particle is 2.64 g/cm<sup>3</sup> and the maximum and minimum void ratios are 0.97 and 0.59 respectively. The cylindrical test specimens were prepared in the way of filling and compacting the sand in a geononwoven stretched tightly in a hollow rigid mould. The relative densities of sands selected in this experiment were at three conditions of  $D_r = 20, 40, 80\%$ . An uniaxial

Table 1 strength of geononwovens

|                               |                      | S-100 | S-200 | S-300 |
|-------------------------------|----------------------|-------|-------|-------|
| tensile strength<br>(N/cm)    | cross direction      | 49.1  | 107.9 | 176.6 |
|                               | transverse direction | 35.3  | 88.3  | 127.5 |
| elongation at breaking<br>(%) | cross direction      | 65    | 65    | 65    |
|                               | transverse direction | 65    | 65    | 65    |

compression test was carried out at the axial compressive strain rate of 1 %. The axial strain was measured by a dial gauge and the mean lateral strain at the middle height of specimen was estimated from the change of its diameter using a pi-meter.

### 3 CONFINING EFFECTS

Under an axial compression of the specimen as shown in Fig.1, the soil mass dilates in the lateral direction and applies pressure to the surface of geotextile if the Poisson's ratio is not zero. Consequently the geotextile resists against its own tensile elongation and maintains radial restraint pressure to the dilatation of soil as shown in Fig.2. The confinement force produced caused by the tensile elongation may depend on the tensile properties of geotextile and the density of soil.

Figure 3 shows the equilibrium of the tensile force of geotextile and inner stress of soil in the radial direction.

$$\sum X_i = (2r \times p_i) - 2T = 0$$

$$p_i = \frac{T}{r} \tag{1}$$

where

- $X_i$  : stress distribution in x-direction
- $r$  : radius of specimen
- $p_i$  : inner radial stress occurred by compression
- $T$  : tensile force of reinforcing material

These confinement by geotextiles is able to generate an apparent cohesion of granular materials in consequence and makes possible to reinforce effectively a cohesionless soil mass.

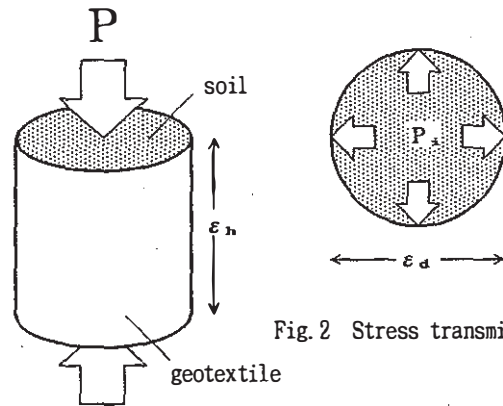


Fig.1 Axial compression

Fig.2 Stress transmission

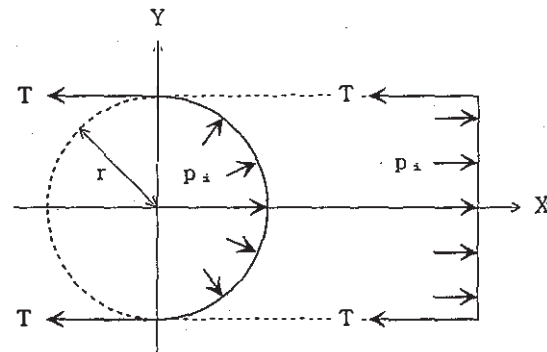


Fig.3 Equilibrium of forces

## 4 RESULTS OF EXPERIMENTS

### 4.1 Uniaxial compression test I

Figure 4 illustrates the influence of relative density of sands on the relations between compressive axial stress and strain. It can be seen that the moduli of deformation and compressive stresses of the specimens increased in proportion to their relative densities.

The effects of tensile properties of geotextiles on the axial stress-strain relationships of the specimens are clearly displayed in Fig.5. It is found that the moduli of deformation of specimens are increased with the increase in the tensile strength of geotextiles.

All of these stress-strain curves demonstrate three stages; namely, the steady linear relations can be obtained in the middle range of strain except of the initial and final ranges in these tests. The implication is that the confining pressure by the

geotextiles depends on the elongation characteristics of geotextiles.

### 4.2 Uniaxial compression test II

Figure 6 shows the effects of relative density on relationships between the compressive stress and radial strain. From this figure it might reasonably be expected that the moduli of deformation between axial stress and radial strain are increased with the increase in the relative densities of sand.

In the similar stress-strain relations shown in Fig.7, it can be observed that the higher tensile strength of geotextiles shows the higher moduli of deformation between axial stress and radial strain.

The typical relations between the axial strain and radial strain are given in Fig.8. It is evident that the relationships show almost linear curves and depend slightly on the relative density.

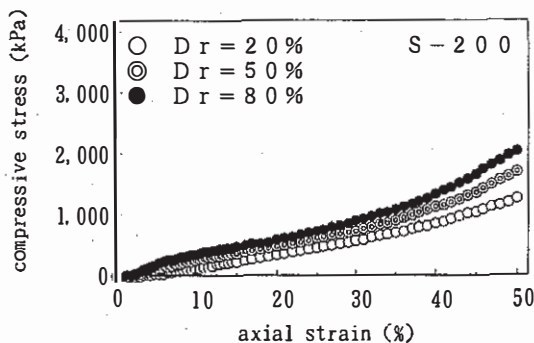


Fig.4 Effects of relative density on compressive stress - axial strain relationships

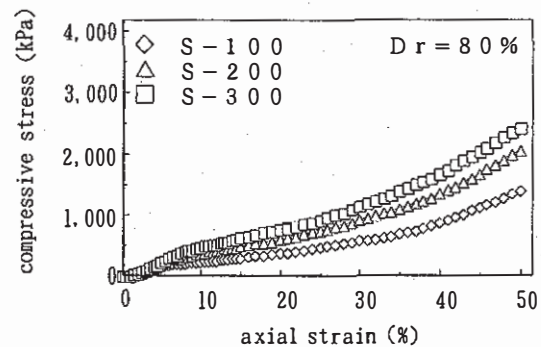


Fig.5 Effects of reinforcing materials on compressive stress - axial strain relationships

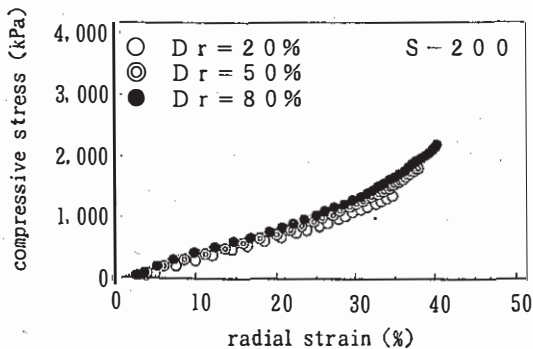


Fig.6 Effects of relative density on compressive stress - radial strain relationships

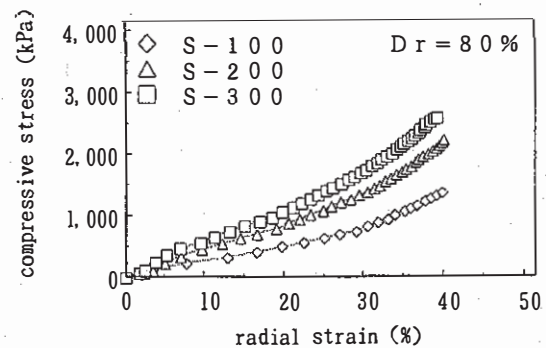


Fig.7 Effects of reinforcing materials on compressive stress - radial strain relationships

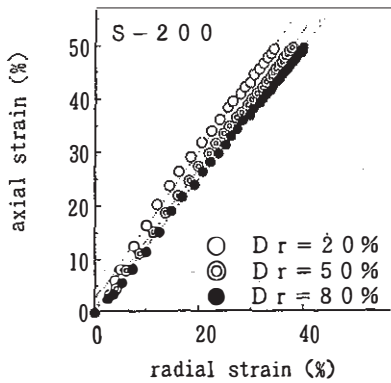


Fig. 8 Axial strain - radial strain relationships

## 5 INTERPRETATION OF TEST RESULTS

### 5.1 Shear strength constants

Figure 9 shows the results of direct shear strength of airdried sand and it can be found that the cohesion is almost zero. The internal friction angles,  $\phi$ , depend on their relative densities;  $\phi = 31^\circ$  at  $Dr = 20\%$ ,  $\phi = 33^\circ$  at  $Dr = 50\%$  and  $\phi = 34^\circ$  at  $Dr = 80\%$ .

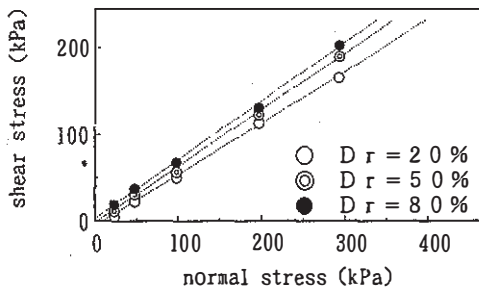


Fig. 9 Effects of relative density on direct shear strength

### 5.2 Apparent cohesion

An estimating method of the apparent cohesion,  $c_{ua}$ , of geotextile-enveloped sand specimen is illustrated in Fig.10. Using the Mohr-Coulomb's failure criteria, the envelope line given by the direct shear test is superimposed on the Mohr's stress circle by the uniaxial compression test. The apparent cohesion component can be obtained as the intercept of the shear stress axis in the way that the envelope line is slid in parallel maintaining

the same angle,  $\phi$ , and makes contact with the stress circle. The apparent cohesion,  $c_{ua}$ , is given in the following equation;

$$c_{ua} = \frac{\sigma}{2} \cos\phi - \left( \frac{\sigma}{2} - \frac{\sigma}{2} \sin\phi \right) \tan\phi \quad (2)$$

Figure 11 shows the relations between the axial compressive stress and the apparent cohesion calculated by the equation (2).

The effects of the relative density on the relationships between the axial strain and the apparent cohesion are demonstrated in Fig.12, and it can be found that the apparent cohesion increases with the increase in the density.

The results of the relation between the axial strain and the apparent cohesion shown in Fig.13, it can be seen that the geotextiles of higher tensile strength displays higher apparent cohesion.

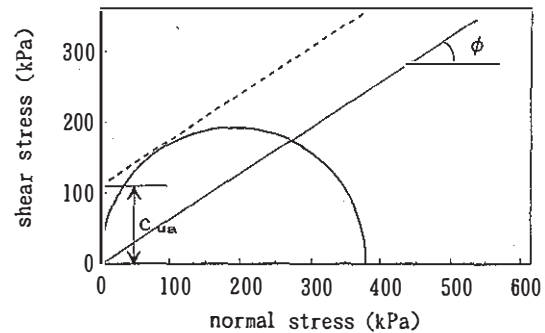


Fig.10 Estimation of apparent cohesion

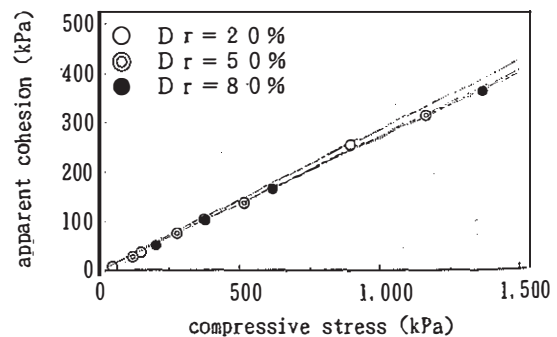


Fig.11 Effects of relative density on apparent cohesion - compressive stress relationships

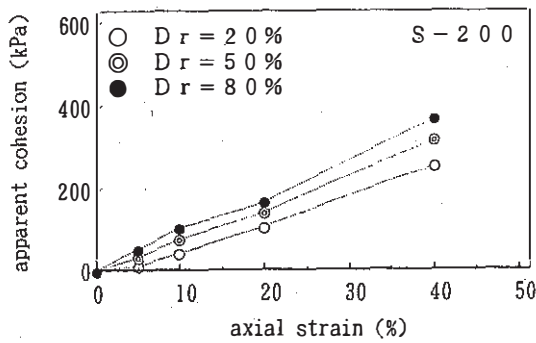


Fig. 12 Effects of relative density on apparent cohesion - axial strain relationships

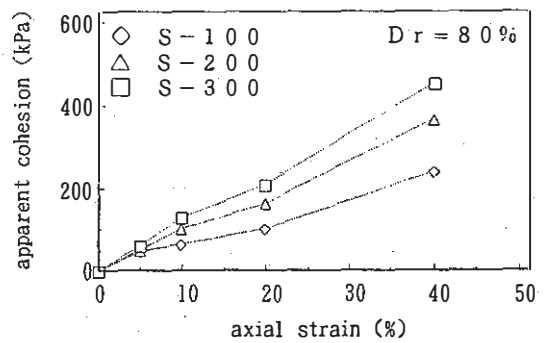


Fig. 13 Effects of reinforcing materials on apparent cohesion - axial strain relationships

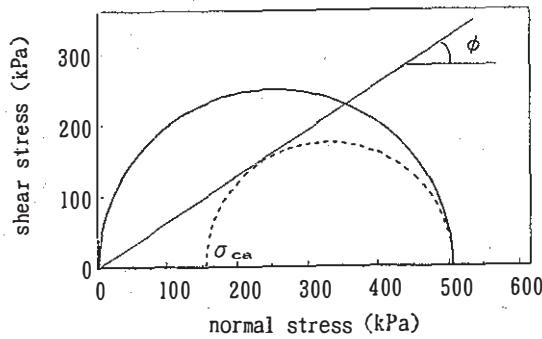


Fig. 14 Estimation of confining effect

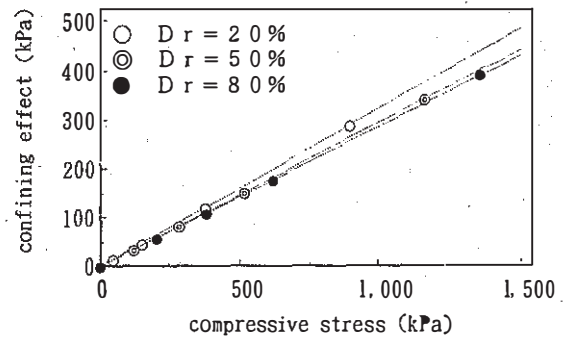


Fig. 15 Effects of relative density on confining effect - compressive stress relationships

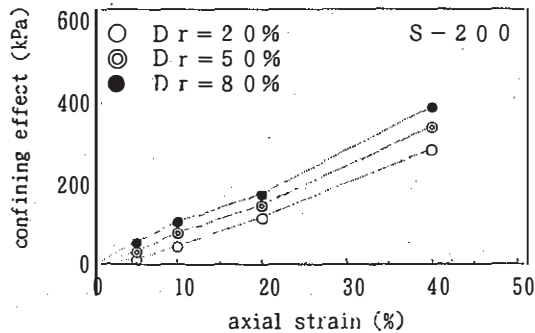


Fig. 16 Effects of relative density on confining effect - axial strain relationships

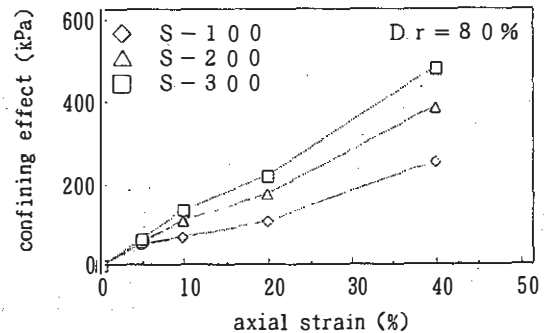


Fig. 17 Effects of reinforcing materials on confining effect - axial strain relationships

### 5.3 Confining effects

Figure 14 shows a schematic layout of estimating method of confining effects. The confining effects expressed in the form of the warrant confining stress,  $\sigma_{ca}$ , can be obtained in the similar way to the apparent cohesion shown in Fig. 10. The apparent confining stress,  $\sigma_{ca}$ , is given in the following equation;

$$\sigma_{ca} = \frac{1 - \sin \phi}{1 + \sin \phi} \cdot \sigma \quad (3)$$

Figure 15 shows the relations between the axial compressive stress and the apparent confining stress calculated by the equation (3).

The effects of the relative density on the

relationships between the axial strain and the apparent confining stress are shown in Fig.16, and it may be seen that the apparent confining stress increases with the increase in the density.

The results of the relation between the axial strain and the apparent confining stress given in Fig.17, it can be found that the the geotextiles of higher tensile strength displays higher apparent confining stress.

## 6 CONCLUDING COMMENTS

A fundamental study using an uniaxial compression tests of geononwovens-enveloped sand was conducted on a cylindrical specimen and the axial and radial stress-strain relationships were investigated. The main results as described below demonstrated the marked improvement of the mechanical characteristics of geocapsulated soil.

- 1) The degree of improvement of geocapsulated soils depends on both the tensile strength and elongation properties of geotextiles and the relative density of soil.
- 2) The stress-strain curves demonstrate three stages against their strain levels. A geotextile used for a confining reinforcement should be utilized at stable range showing a linear stress-strain relation in the middle range of strain, because the breakage of geotextile itself or its seaming may be easily occurred at the final stage.
- 3) The mobilized confining pressure and deformation restraint of geotextiles can be expressed in the form of an apparent cohesion or an apparent confining stress.
- 4) The estimation methods of apparent cohesion and confining stress of geocapsulated granular soil were presented.

## REFERENCES

- R.M.Koerner : Designing with Geosynthetics, 3rd Ed., Prentice Hall, 1994
- Ed. by R.Veldhuijzen van Zanten : Geotextiles and Geomembranes in Civil Engineering, A.A.Balkema, 1986